Development 126, 5409-5420 (1999)
Printed in Great Britain © The Company of Biologists Limited 1999
DEV7758

double-time is identical to *discs overgrown*, which is required for cell survival, proliferation and growth arrest in *Drosophila* imaginal discs

Olav Zilian[1,*], Erich Frei[1], Richard Burke[2], Doris Brentrup[1,‡], Thomas Gutjahr[1], Peter J. Bryant[3] and Markus Noll[1,§]

[1]Institute for Molecular Biology and [2]Zoological Institute, University of Zürich, CH-8057 Zürich, Switzerland
[3]Developmental Biology Center, University of California, Irvine, California 92697, USA
*Present address: ISREC, Chemin des Boveresses 155, CH-1066 Epalinges, Switzerland
‡Present address: Max-Planck-Institute for Biophysical Chemistry, Department of Molecular Cell Biology, D-37077 Göttingen, Germany
§Author for correspondence (e-mail: noll@molbio.unizh.ch)

Accepted 10 September; published on WWW 9 November 1999

SUMMARY

We have isolated the *discs overgrown* gene of *Drosophila* and shown that it encodes a homolog of the Casein kinase Iδ/ε subfamily and is identical to the *double-time* gene. However, in contrast to the weak *double-time* alleles, which appear to affect only the circadian rhythm, *discs overgrown* alleles, including bona fide null alleles, show strong effects on cell survival and growth control in imaginal discs. Analysis of their phenotypes and molecular lesions suggests that the Discs overgrown protein is a crucial component in the mechanism that links cell survival during proliferation to growth arrest in imaginal discs. This work provides the first analysis in a multicellular organism of Casein kinase Iδ/ε functions necessary for survival. Since the amino acid sequences and three-dimensional structures of Casein kinase Iδ/ε enzymes are highly conserved, the results suggest that these proteins may also function in controlling cell growth and survival in other organisms.

Key words: *discs overgrown*, Casein kinase Iδ/ε, Cell survival, Growth arrest, Imaginal discs, *Drosophila melanogaster*

INTRODUCTION

An important problem in the development of an organism is how regulation of cell proliferation is coupled to the organization and patterning of the developing organs and tissues to determine their proper size and shape. An ideal system to study this question is the imaginal discs of *Drosophila*, which develop into the external structures of the adult head, thorax, and genitalia (for a review, see Edgar and Lehner, 1996). Imaginal discs of 10-50 cells begin to proliferate exponentially after first-instar larvae have hatched and begun to feed. Proliferation continues up to the late third larval instar when the number of cells has increased about 1000-fold, after which the discs differentiate into adult structures during metamorphosis. During the growth period, morphogens, including the protein products of the *decapentaplegic* (*dpp*) and *wingless* (*wg*) genes, are secreted from localized sources and organize the patterning of the discs (Lecuit et al., 1996; Nellen et al., 1996; Zecca et al., 1996). Morphogens also stimulate cell proliferation although little is known about the mechanisms by which they do this (Edgar and Lehner, 1996; Serrano and O'Farrell, 1997). There is no obvious correlation between morphogenetic events and cell proliferation, which occurs in clusters throughout discs, possibly because proliferation depends on a complex pattern of superimposed morphogenetic signals and/or on mitogens distinct from morphogens.

To analyze the question of how cell proliferation is regulated in imaginal discs, we have searched for mutants defective in growth control by two approaches. In the first approach, we searched for recessive mutants in which mutant mitotic clones displayed excessive growth. Identification of one such mutation resulted in the isolation of the *warts* (*wts*) gene. Loss of this gene results not only in overproliferation but also in apical hypertrophy of epithelial cells, suggesting that mitosis is at least partially decoupled from cellular growth in *wts* mutants (Justice et al., 1995). In the other approach, we analyzed mutants showing excess cell proliferation in imaginal discs, and this resulted in the identification of the *discs overgrown* (*dco*) gene whose phenotype showed, at least for one allele, hyperplastic growth of imaginal discs. These discs showed defects in gap-junctional communication as evident from a dramatic reduction in dye coupling of imaginal disc cells (Jursnich et al., 1990).

To analyze the molecular basis for its mutant phenotypes and to investigate its role in cell proliferation, we have now identified and isolated the *dco* gene. In addition, several new hypomorphic and amorphic *dco* alleles were obtained and have been analyzed with respect to their phenotypes and molecular lesions. We find that *dco* encodes a homolog of human casein kinase Iδ/ε (CKIδ/ε) and is identical to the previously cloned *double-time* (*dbt*) gene (Kloss et al., 1998), which plays an important role in controlling the period of the circadian rhythm (Kloss et al., 1998; Price et al., 1998). Our analysis of the

phenotypes of various *dco* mutants, including heteroallelic combinations of strong and null alleles, suggests that *dco* is required for inhibition of apoptosis during cell proliferation as well as for growth arrest in imaginal discs.

MATERIALS AND METHODS

General procedures

Standard procedures, such as isolation and Southern blot analysis of genomic DNA, construction and screening of genomic libraries in λDASH II (Stratagene) and of a 4- to 8-hour embryonic cDNA library in the λUNI-ZAP XR vector (Stratagene), and isolation of poly(A)$^+$ RNA, were carried out essentially as described (Maniatis et al., 1982; Frei et al., 1985; Kilchherr et al., 1986; Fu and Noll, 1997). DNA sequences flanking P-element insertions were recovered by plasmid rescue (Pirrotta, 1986). All DNA sequences were determined on both strands by the dideoxynucleotide method with a DNA sequencer Model 373A using dye terminators (Applied Biosystems Inc.).

Using the 3.2, 0.6 and 3.8 kb genomic *Eco*RI fragments of *dco* (Fig. 6B) as probes, 15 *dco*-cDNAs were isolated from an embryonic cDNA library. The length of the three largest cDNAs, c193-1.11.13-16, c193-1.11.13-17 and c193-1.11.13-19 is 3.8 kb, which is close to full-length as judged from northern blot analysis (data not shown). This conclusion is further supported by the observation that their 5′ ends and that of an additional cDNA, c193-1.11.12-4, are located within only 14 bp. Sequence analysis of the 3′ ends of the isolated cDNAs reveal two clusters of polyA addition sites, which include six cDNAs each and are located less than 50 bp downstream of canonical polyA addition signals AATAAA, whereas the remaining three cDNAs end 0.4 kb and 1.1 kb upstream of the longest cDNAs and less than 50 bp downstream of the probable polyA addition sites AATTAA, CATAAA, and TATAAA, which deviate at single positions from the canonical sequence (Fig. 6B).

Generation of deficiencies and P-element mutagenesis

Large deficiencies used to map *dco*, such as *Df(3R)A177der20* and *Df(3R)A177.X1* (Fig. 6A), were generated by X-ray-induced losses of the *ry*$^+$ P-element insertion *P[lArB]A177* (kindly provided by Hugo Bellen, Baylor College of Medicine, Houston, TX) as described by Justice et al. (1995). The deficiencies *Df(3R)PGX4* and *Df(3R)PGX8* (kindly provided by Judy Lengyel and formerly called *Df(3R)EGX4* and *Df(3R)EGX8*) were generated by F. Pignoni, J.R. Merriam and J.A. Lengyel in a screen of X-ray-induced lethals over the *tll*^{g} deficiency (Pignoni et al., 1990). The duplication *Dp(3;1)150P* has been derived as an X-ray-induced deletion of *ca*$^+$ (Frisardi and MacIntyre, 1984) from *Dp(3;1)B152* (Kankel and Hall, 1976), and was combined with the terminal third chromosome deficiency of *T(Y;3)A113* to generate the synthetic deficiency *Df(3R)A113 Dp(3;1)150P* (Kongsuwan et al., 1986; Strecker et al., 1988). Portions of the third chromosome juxtaposed to X- or Y-chromosome heterochromatin in *Dp(3;1)150P* inactivates *dco* on this duplication as we have shown by its derepression through supernumerary Y chromosomes (Lindsley et al., 1960).

To obtain small deletions of the *dco* gene, the P-element insertion *P3670* (*P{ry*$^{+t7.2}$*=PZ}l(3)3670*, kindly provided by the Berkeley Drosophila Genome Project), shown to be in close proximity to *dco* by recombination mapping, was mobilized in *ry*^{506} *P3670/ry*^{506} *Sb P[ry*$^+$ *Δ2-3]* males (Robertson et al., 1988) and their *ry* offspring, which had lost the P element, were screened for imprecise excisions by complementation with *P3670* and *dco*. One deficiency, *Df(3R)dco*$^{i3\text{-}193}$, which uncovers *dco* but complements *P3670*, and several deficiencies deleting both loci were recovered. In addition, several small deficiencies that complemented with *dco* but did not complement with *P3670* were obtained (Fig. 6B).

The P-element insertion allele *dco*^{P103} and the deficiency *Df(3R)PH3* were recovered over a small deficiency uncovering the lethality of the *P3670* insertion, but complementing *dco* (see above), as *ry*$^+$ offspring from *ry*^{506} *P3670/ry*^{506} *Sb P[ry*$^+$ *Δ2-3]* males (Tower et al., 1993; Zhang and Spradling, 1993). Complementation tests and molecular analyses showed that the deficiency *Df(3R)PH3* has retained a P element that could be recovered by plasmid rescue (Pirrotta, 1986) although it has lost the *ry*$^+$ marker.

Rescue of *dco* mutants

For rescue of *dco* mutants, a 13.1 kb genomic fragment including the entire *dco* gene (Fig. 6B) was cloned into the *Not*I site of the P-element vector pCasPeR 4 (Thummel and Pirrotta, 1992). The upstream *Not*I site is a genomic site while the downstream *Not*I site is derived from the λ DASH II cloning site of the genomic library used. The P-element rescue construct was injected into *w*^{1118} embryos and G1 *w*$^+$ tranformants crossed with *dco* mutants to establish several *y w*; *P[w*$^+$ *dco*$^+$*]*; *dco* stocks. The P-element rescue construct rescues all *dco* alleles as well as the *P3670* lethal insertion into the adjacent distal transcription unit *X94917* (Fig. 6B), of which it includes the entire open reading frame. We have not tested if the mutant circadian rhythm phenotypes of the two reported *dbt* alleles (Kloss et al., 1998) of *dco* are rescued by our *dco*$^+$ transgene and hence do not know whether it includes all enhancers.

Clones mutant for *dco*

Marked *dco* mutant clones in wing discs were generated by subjecting *y w hsp70-flp omb-lacZ* or *y w hsp70-flp brk-lacZ/y w* or *Y*; *FRT82 dco*^{le88} or *FRT82 dco*^{3}*/FRT82 2πM* larvae to FLP-mediated recombination (Xu and Rubin, 1993) induced by heat shock (30 minutes at 33°C). Induction of πM expression, dissection and staining for πM and β-gal was as described (Nellen et al., 1996). Marked *y*; *dco*^{3} clones in adults were produced in *y hsp70-flp/y w* or *Y*; *FRT82 dco*^{3}*/FRT82 πM y*$^+$ larvae in the same way. In case of induction of *dco M*$^+$ clones in a *M*/+ background, the *FRT82 2πM* chromosome or the *FRT82 πM y*$^+$ chromosome was replaced by the *FRT82 M(3)w*^{124} *πM y*$^+$ chromosome.

Histology and electron microscopy

Imaginal discs were dissected in PBS and fixed in 2% glutaraldehyde. The tissue was washed several times in 0.1 M cacodylate buffer, pH 7.2, containing 8% sucrose, postfixed in osmium tetroxide, embedded in plastic and sectioned for light and electron microscopy. Thick sections were stained with toluidine blue and thin sections stained with lead citrate and uranyl acetate.

RESULTS

Reduced growth, loss, or overgrowth of imaginal discs caused by *dco* mutations

Since the original description of *dco* (Jursnich et al., 1990) many new alleles of the gene have been produced by various mutagenic procedures. We therefore analyzed the phenotypes of these new alleles as well as of some new deficiencies and of the few alleles described earlier (Jursnich et al., 1990), in homozygotes and heteroallelic combinations. The effects of *dco* mutations on imaginal discs are seen most clearly in the wing disc, since this disc is fairly flat and any morphological or growth abnormalities are easily detectable in whole mounts (Table 1; Fig. 1). Most genotypes involving alleles other than *dco*^{3} or *dco*^{P1447} show various degrees of abnormality, ranging from complete absence of discs to apparently normal discs (Fig. 1A-F). In intermediate cases, the folding pattern of the epithelium is very abnormal, and the discs often show a dark, granular zone

Table 1. *dco* complementation matrix

	3	*2*	*18*	*le 88*	*i3-193*	*PCX8*	*Ph3*	*P538*	*P1396*	*P915*	*P103*	*P1447*
3	L/P; Og											
2	L/P; Og	Emb										
18	L/P; Og	L/P; DI	Emb									
le 88	LP*; Og	L/P	L	L; DI								
i3-193	LP*; Og	L/P; Ab	L	L; DI	Emb							
PGX8	LP*; Og	L/P	L	L	L	Emb/EL						
PH3	L/P*; Og	L/P; Ab	L	L	L	L	Emb					
P538	LP*; Og	L/P; Sm	L	L;Dl	L	L	L	L				
P1396	LP*; Og	L/P; Ab	L/P; Dl	L/P; Dl	L/P; Dl	L/P; Dl	L/P; Dl	L/P; Dl	L/P; Dl			
P915	LP*; Og	E/LP*; Ab	L/P; Dl	L/P; Sm	L/P; Sm	L/P; Ab	L; Sm	L/P; Sm	L/P; N	L/P; Ab		
P103	LP*; Og	A^1; N	L/P; Ab	LP; Ab	A^3;Ab	L; Sm	L; Sm	A^3;Ab	E/LP; Ab	A; N	L/P	
P1447	A^2	A^4	A^4,A^3	A^4	A^4	A^4,A^2	NT	A^4	A^4	A	A^4	NT

Phenotypes of homo- and heteroallelic combinations of EMS- (*3*, *2*, *18*, *le88*) and P element-induced (*P538*, *P1396*, *P915*, *P103*, *P1447*) *dco* alleles and of *dco* deficiencies (*i3-193*, *PGX8*, *PH3*) are listed in a complementation matrix according to their lethal periods (Emb, embryogenesis; Emb/EL, embryogenesis or early larval stages; L, larval stages; L/P, larval or early pupal stages; E/LP, early or late pupal stages; LP, late pupal stage), disc phenotypes (Dl, discless; Sm, small discs; Ab, abnormal discs with granular zone and abnormal folding; Og, overgrown disc; N, normal disc) and late pupal (pharate adults) and adult phenotypes (*, late pupal lethal with typical dco^3 phenotype (swollen tarsi, or swollen tarsi with head defects); LP, late pupal lethal with normal phenotype; A^1, adult viable with expanded wings and leg outgrowths (Fig. 3); A^2, adult viable with reduced eyes, extra vibrissae, and expanded wings; A^3, adult viable with narrow wings; A^4, adult viable with reduced eyes, slightly disordered facets, and minor wing vein defects; A, adult viable with normal phenotype). Note that (i) some homozygous combinations (*2*, *18*, *i3-193*, *PGX8*, *PH3*, *P538*) die during embryogenesis because of linked embryonic lethals different from *dco*; (ii) the P-element insertion chromosome *P103* is still associated with the *P3670* insertion, from which it has been derived by local hop, and hence is a double mutant for the two neighboring loci *dco* and *P3670* (or *X94917*), which are both uncovered by the deficiencies *PGX8* and *PH3* (Fig. 6A); and (iii) the P-element insertion chromosome *P1447* carries a closely linked lethal mutation, which is uncovered by the deficiency *Df(3R)PGX4* (J. Szidonya, personal communication, and our own observations; Fig. 6A), but not caused by the insertion of a rescuable P element. Two combinations have not been tested (NT). Discless phenotypes (Dl) result from a progressive degeneration of discs during late larval stages and are distinguishable from small-disc phenotypes (Sm) whose discs do not degenerate completely, even after prolonged larval life (7-9 days at 25°C). Heteroallelic combinations of *P1447* with alleles other than dco^3 exhibit adult phenotypes (reduced eyes and/or slightly disordered facets, rare excess vibrissae, defects in veins and shape of wings) whose penetrance and expressivity depend strongly on the allelic combination (relatively high penetrance of eye phenotype in *P1396*, *P538*, *PGX8*, and *18*; relatively high penetrance of wing phenotype in *18* and *PGX8*) and are frequently much higher in females than in males. The EMS-induced alleles form an allelic series with *le88* (null) > *18* > 2. The P-element insertion alleles may also be ordered into a series of decreasing strength: *P538* > *P1396* > *P915* > *P103* > *P1447*.

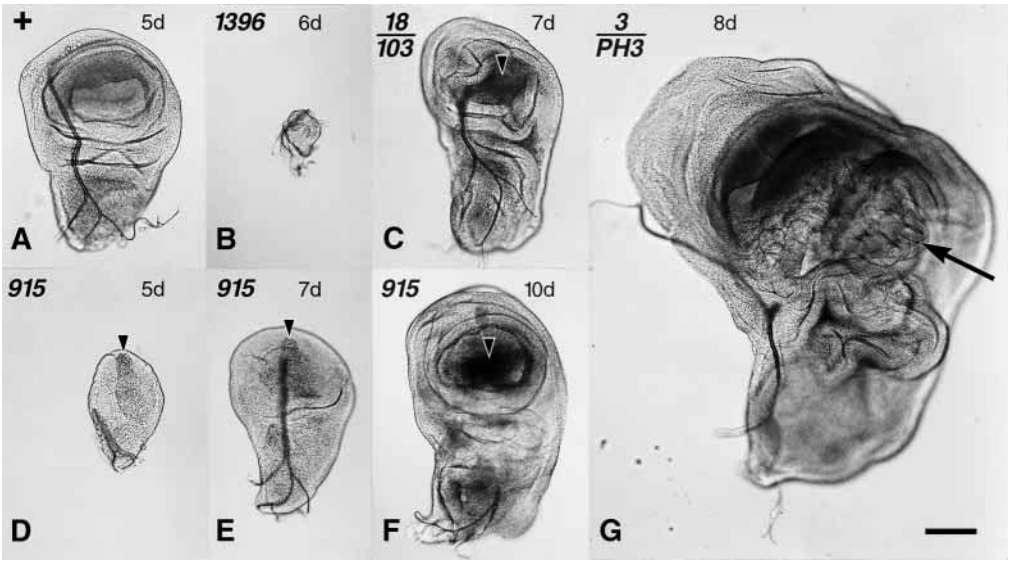

Fig. 1. Reduction and overgrowth of imaginal wing discs in *dco* mutants. (A) Wild-type, 5 days after oviposition; (B) dco^{P1396} homozygote, 6 days after oviposition – highly reduced discs; discs have completely degenerated by this time in most homozygous dco^{P1396} larvae, which therefore are listed as discless in Table 1. (C) dco^{18}/dco^{P103}, 7 days after oviposition – abnormal folding pattern and dark, granular area in wing pouch (arrowhead); (D,E,F) dco^{P915} homozygotes, 5, 7, and 10 days after oviposition – abnormal folding pattern and dark, granular area in wing pouch (arrowheads); (G) $dco^3/Df(3R)PH3$, 8 days after oviposition – highly overgrown disc with a central area (arrow) showing highly folded epithelial layers. Scale bar, 100 μm.

in the wing pouch region (Fig. 1C-F). These phenotypes are produced by EMS-induced alleles (dco^2, dco^{18} and dco^{le88}), P-element insertions (dco^{P103}, dco^{P538}, dco^{P915} and dco^{P1396}), and deletions induced by X-ray (*Df(3R)PGX8* and, e.g., *Df(3R)A177der21*) or P-element excision ($dco^{i3\text{-}193}$, *Df(3R)PH3*). All of the genotypes giving a discless or small-disc phenotype cause lethality in the embryo, larva or pupa before adult differentiation (Table 1). As will be shown below, these phenotypes result from combinations of strong loss-of-function *dco* alleles. Most of those genotypes that display an abnormal disc phenotype, caused by combinations of weaker *dco* alleles, also lead to death at some time before adult differentiation;

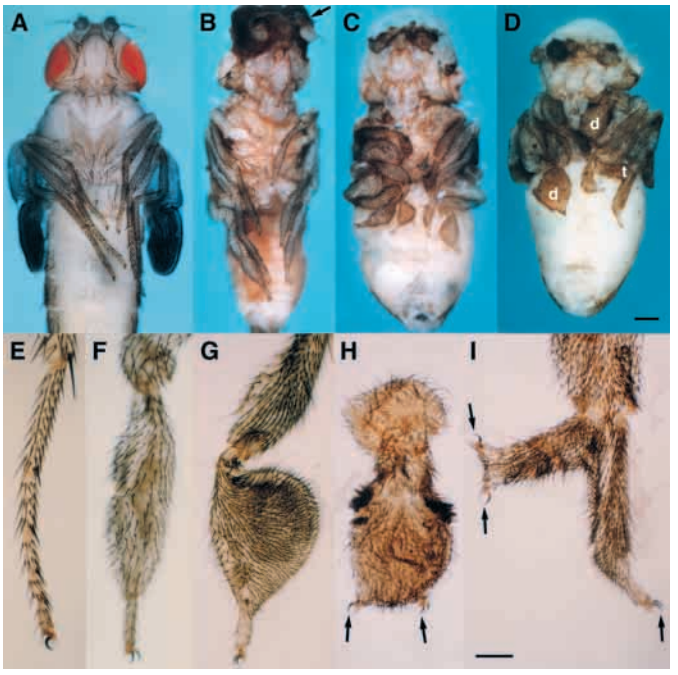

Fig. 2. Growth abnormalities in the pharate adults produced by heteroallelic *dco*^{3} combinations. (A) Wild-type pharate adult. (B) *dco*^{3}/*dco*^{P1396} pharate adult showing expanded tarsi and overgrown ptilinum associated with reduced eyes (arrow). (C) *dco*^{3}/*Df(3R)PGX8* pharate adult showing overgrown 'spadefoot' tarsi. (D) *dco*^{3}/*Df(3R)PGX8* pharate adult showing two 'spadefoot' tarsi, two distally duplicated tarsi (d) and one triplicated tarsus (t). (E) Normal tarsus from wild-type pharate adult. (F) Expanded tarsus from *dco*^{3}/*dco*^{P1396} pharate adult. (G) 'Spadefoot' tarsus from *dco*^{3}/*Df(3R)PGX8* pharate adult. (H) Duplicated tarsus with sex combs (arrows show claws) from *dco*^{3}/*Df(3R)PGX8* pharate adult. (I) Triplicated tarsus (arrows show claws) from *dco*^{3}/*Df(3R)PGX8* pharate adult. Scale bar, 200 μm (A-D) or 100 μm (E-I).

however, some allow survival to late pupae, and in one case (*dco*^{2}/*dco*^{P915}) the pupae show a phenotype including expanded tarsi that is otherwise typical of *dco*^{3} combinations (see below).

In *dco*^{3} homozygotes or heteroallelic combinations of *dco*^{3} with any of the other known *dco* alleles or deficiencies, the larval period is prolonged by many days. During this time, the imaginal discs grow continuously to several times the wild-type final size (Fig. 1G; Table 1). The mutant discs retain their epithelial structure, hence the overgrowth should be classified as hyperplastic rather than neoplastic. The wing discs develop a central region of excess growth in which the epithelial folds are thinner and more convoluted than normal, as noted previously (Jursnich et al., 1990). The larval period is also prolonged and growth of discs slowed down in homozygous or heterozygous combinations of *dco* alleles that eventually produce normal size discs with abnormal folding (Fig. 1C-F; Table 1).

dco^{3} pharate adults show morphogenetic aberrations including duplicated structures

Many heteroallelic combinations with *dco*^{3} allow survival to late pupal or pharate adult stage (i.e., fully differentiated adults, which die without leaving the pupal case). These animals typically have swollen tarsal segments (Fig. 2B-D,F) and abnormal heads in which the ptilinum (a cuticular balloon on the front of the head that is inflated by blood pressure to push open the door of the puparium in order to allow the adult to emerge, and is then retracted) appears enlarged and fails to retract (Fig. 2B). Eyes are often missing, and are sometimes replaced by duplicated antennae. Excess bristles are often seen on the antennae. One genotype (*dco*^{3}/*Df(3R)PGX8*) produces greatly enlarged tarsi giving a 'spadefoot' appearance (Fig. 2C,G). Most notably, some of the legs in this genotype show distally duplicated or even triplicated ventralized structures, such as duplicated sex combs and claws (Fig. 2D,H,I). The wings of these animals fail to expand and therefore any pattern abnormalities are difficult to discern and could only be analyzed in clones (see below).

Fig. 3. Localized overgrowth produced in legs of *dco*^{2}/*dco*^{P103} adults. (A) Femur; (B) tibia; (C,D) tarsus. Scale bar, 100 μm.

Adult phenotypes of weak *dco* mutants

The allele *dco*^{P103} seems to have unique properties: *dco*^{P103}/*dco*^{2} produces normal imaginal discs and allows survival to adulthood (Table 1), but the adults show expanded wings and localized outgrowths from the antennae and the distal leg segments (Fig. 3). Combinations of *dco*^{P103} with *dco*$^{i3\text{-}193}$ or *dco*^{P538} produce abnormal imaginal discs but allow survival to adulthood, and the adults have abnormally narrow wings. One other combination (*dco*^{P103}/*dco*^{P915}) allows survival to adulthood with no apparent abnormalities.

Another set of phenotypes is seen in surviving adults heteroallelic with the P-element insertion *dco*^{P1447}. Thus, *dco*^{P1447}/*dco*^{3} shows several head abnormalities including excess vibrissae, enlarged antennae and a widened prefrons often associated with reduced eyes, as well as an expanded wing with excess vein material along vein 2 and often an incomplete posterior cross-vein (Table 1). The head phenotype is also seen at low frequency in *dco*^{P1447}/*Df(3R)PGX8*. In contrast, *dco*^{P1447}/*dco*^{18} adults have reduced wings, and they often also show incomplete posterior veins (Table 1). Heteroallelic combinations of *dco*^{P1447} with alleles other than *dco*^{3} exhibit an adult phenotype whose penetrance and expressivity depend strongly on the allelic combination and are frequently much higher in females than in males (see legend to Table 1).

dco^{-} clones are growth-inhibited and fail to survive in discs

Null or strong *dco* alleles show greatly reduced cell

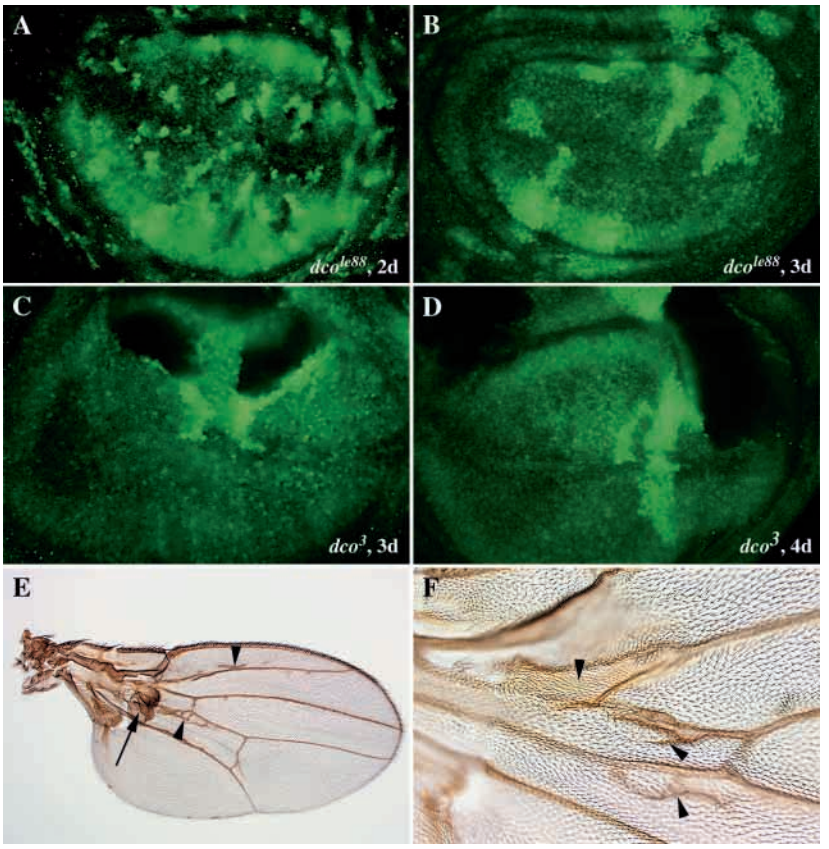

Fig. 4. Growth inhibition of *dco*$^{-}$ clones and overgrowth of *dco*^{3} clones. (A-D) Mutant *dco* clones are shown in wing pouch portions of wing discs from wandering third-instar larvae with anterior to the left and ventral side down. Mitotic *dco*^{le88} (A,B) and *dco*^{3} clones (C,D) were induced 2 (A), 3 (B,C), or 4 days (D) before staining for πM (green). Clones mutant for *dco* are marked by the absence of πM whereas their twin clones express twice as much πM as the heterozygous background. (E,F) Phenotype of *y*; *dco*^{3} clones, induced in 1-2 day-old (E) or 2-3 day-old larvae (F), are shown in an adult wing (E) or in an enlarged view of the proximal portion of a different wing (F). The arrow in E points to a large outgrowth of a *dco*^{3} clone while arrowheads in E and F indicate additional vein tissue formed by *dco*^{3} clones.

proliferation in imaginal discs and thus produce very small discs that eventually degenerate because of apoptosis (see below) and give rise to the discless phenotype (Table 1). Some *dco*^{3} phenotypes show partially duplicated leg structures (Fig. 2D,H,I) that are reminiscent of phenotypes produced by leg disc clones that cannot receive the Dpp signal (Jiang and Struhl, 1996; Theisen et al., 1996). To test whether these effects on growth and apoptosis of strong *dco* alleles are clone- or disc-autonomous and caused by a defect in Dpp signaling, we induced mitotic clones of *dco*^{le88}, which is a null allele (see Appendix), in imaginal discs at various times during larval development and examined whether absence of *dco* activity in these clones had an effect on cell growth or survival, the activity of Dpp target genes, or the adult phenotype.

Inspection of wing discs from wandering third-instar larvae showed that *dco*$^{-}$ clones, induced relatively late (2 days before analysis) and marked by the absence of πM expression (Xu and Rubin, 1993), can be observed but are less than half the size of their twin clones which consist of up to about 16 cells and express twice the level of πM compared with the surrounding heterozygous π*M* cells (Fig. 4A). In contrast, nearly no cells of *dco*$^{-}$ clones induced one day earlier are detectable while their

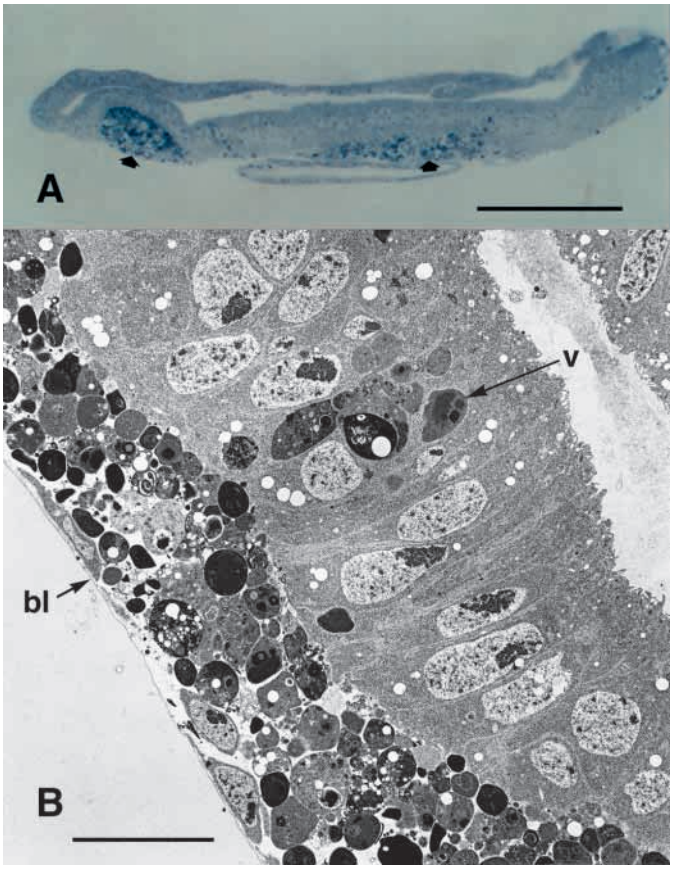

Fig. 5. Localized apoptotic cell death in 7-day *dco*^{18}/*dco*^{P103} imaginal wing discs. (A) Light micrograph of a toluidine blue-stained plastic-embedded wing disc section showing apoptotic cells (arrows). Scale bar, 100 μm. (B) Electron micrograph of wing disc section. Note vesicle (V) representing part of a cell in the process of apoptosis. The remains of dead cells are accumulated basal to the epithelium, under the basal lamina (bl). Scale bar, 10 μm.

twin clones are of the expected normal size (Fig. 4B). When clones are induced 4 days before analysis, no *dco*$^{-}$ cells are observed and twin clones consist of hundreds of cells (not shown; but cf. Fig. 4D). Clearly, cells that lack a functional *dco* gene are unable to undergo continued growth and cell proliferation and die after only two or three divisions. Similar results were obtained for *dco*$^{-}$ *Minute*$^{+}$ clones in a *Minute* (*M*) background (not shown). It thus appears that these clones do not die because of a growth disadvantage with respect to competing wild-type cells as is characteristic for *M* clones in a wild-type background (Morata and Ripoll, 1975; Simpson, 1979). The results further demonstrate that the growth inhibition and apoptosis of *dco*$^{-}$ cells is cell-autonomous, which suggests that *dco*$^{-}$ cells are unable to respond to a signal required for growth or survival.

Consistent with the above findings, no *dco*$^{-}$ clones marked by the absence of the *yellow* (*y*) gene survived to adulthood either in a wild-type or heterozygous *M* background unless they were induced in imaginal discs shortly before pupariation. Such very late-induced clones occasionally include surviving *y* bristles whose shafts are absent or considerably smaller than those of *M* mutants (not shown). In most cases, the loss of *dco*$^{-}$ clones does not affect the final adult pattern, probably because surrounding cells compensate for the loss by extra proliferation. Occasionally, if many clones are induced very early in larval discs, compensation is incomplete and the bristle pattern is disturbed or, in extreme cases, the scutellum is severely affected. In contrast, clones derived from *dco*$^{-}$/*dco*$^{+}$ larval histoblasts, in which mitotic recombination had been induced, survive as *y* patches on the adult abdominal cuticle (not shown). This is not surprising considering that histoblasts grow tremendously in size, about 60-fold, during larval stages in the absence of cell proliferation before the last 3-4 cell divisions occur during the pupal stage (Madhavan and Schneiderman, 1977). Hence, both the limited growth of *dco*$^{-}$ cells observed in larval discs and the survival of histoblast clones to adulthood can be explained by the perdurance of wild-type Dco protein in the mutant cells.

Since some of the *dco*^{3} phenotypes are reminiscent of phenotypes resulting from clones of cells that cannot respond to the Dpp signal, we examined the expression of the Dpp target genes *brk-lacZ*, which is negatively regulated by Dpp (Campbell and Tomlinson, 1999), and *omb-lacZ* (Sun et al., 1995), which is activated by Dpp, in *dco*$^{-}$ clones of third-instar wing discs. We find only a slight reduction in *omb-lacZ* expression shortly before cells die, while *brk-lacZ* remains fully repressed (not shown). Since the activity of these target genes is clearly altered in similar clones mutant for the Dpp receptor (Burke and Basler, 1996), it follows that *dco* is not essential for the transduction of the Dpp signal, and effects of *dco* on growth are not mediated by Dpp.

The *dco*^{3} mutation causes overgrowth autonomously in genetic mosaics

In order to test the clonal autonomy of the *dco*^{3} overgrowth phenotype, we generated *dco*^{3} clones at various larval stages as for the *dco*^{le88} null allele. Again, no effect on Dpp target genes is detectable in such clones of discs from wandering third-instar larvae (not shown). However, in contrast to *dco*^{le88} clones, *dco*^{3} clones not only continue to grow and proliferate but fail to stop growth when the discs have reached their normal size (Fig. 4C,D). Such clones are larger than their twin clones, although the size of *dco*^{3} cells is not affected (not shown), and exhibit moderate overgrowth (Fig. 4C,D). This moderate overgrowth is not due to accelerated cell proliferation in *dco*^{3} cells because the ratios of the sizes of wild-type clones induced at various times before analysis and those of *dco*^{3} clones induced at the same times before analysis are the same (Fig. 4C,D and results not shown). In agreement with the above results, *dco*^{3} clones survive to adulthood and show excess tissue as revealed, for example, in wings and especially in the wing vein regions (Fig. 4E,F). No excess tissue appears in *dco*^{3} adult clones originating from histoblasts, presumably because of the perdurance of the wild-type Dco protein.

If more clones are induced, the larval life is considerably prolonged by up to two days and the clones exhibit massive overgrowth such that the discs are clearly enlarged (not shown). Such animals die as pharate adults like *dco*^{3} mutants and exhibit almost identical disc and pharate adult phenotypes. These results show that *dco*^{3} disc cells are still able to transduce growth and survival signals. Moreover, since most larval tissue does not proliferate after clone induction, it follows that *dco*^{3} disc cells are defective in responding to the signal that stops growth of the mature larval disc. This conclusion is further consistent with the recessive nature of the *dco*^{3} allele (see below) and its cell-autonomous effect on growth arrest. In addition, as pupariation is delayed in such mosaic animals, we conclude that *dco*$^{+}$ appears to be required in discs for the proper timing of pupariation.

Apoptosis caused by *dco* mutations

The abnormal imaginal discs produced in many *dco* genotypes have a localized area that appears granular and dark in transmitted light (Fig. 1), a characteristic of degeneration as previously reported in overgrowing *dco* imaginal discs (Jursnich et al., 1990). Studies by both light and electron microscopy showed clearly that, in these areas, individual cells undergo apoptosis as evident from the occurrence of fragmentation, condensation and basal extrusion (Fig. 5). The basally extruded fragments accumulate under the basal lamina (Fig. 5). This type of cell degeneration is typical of apoptosis and associated with mutations that cause tissue loss in imaginal discs (e.g., O'Brochta and Bryant, 1983).

Identification and isolation of the *dco* gene

The *dco* gene was previously mapped to the tip of the right arm of the third chromosome, distal to *tailless* (*tll*) (Jursnich et al., 1990). Furthermore, it was known to reside distal to *Df(3R)A177der20* and thought to lie proximal to the breakpoint of *Dp(3;1)150P* because *dco* mutations are not complemented by the synthetic deficiency *Dp(3;1)150P*; *Df(3R)A113* (Jursnich et al., 1990). The latter conclusion turns out to be incorrect since part of the translocation of *Dp(3;1)150P* is inactivated as a result of its juxtaposition to sex chromosome heterochromatin (see Materials and Methods).

In order to map *dco* more precisely, several X-ray-induced deficiencies of a nearby P-element insertion, *P(lArB)A177* (Justice et al., 1995), and another deficiency of this region, *Df(3R)PGX8* (kindly provided by J. Lengyel), were tested for complementation with *dco* and each other (Fig. 6A). In addition, the deficiencies were mapped with respect to several loci of the relevant chromosome region that complemented *dco*, including the recessive lethal P-element insertions *P990*

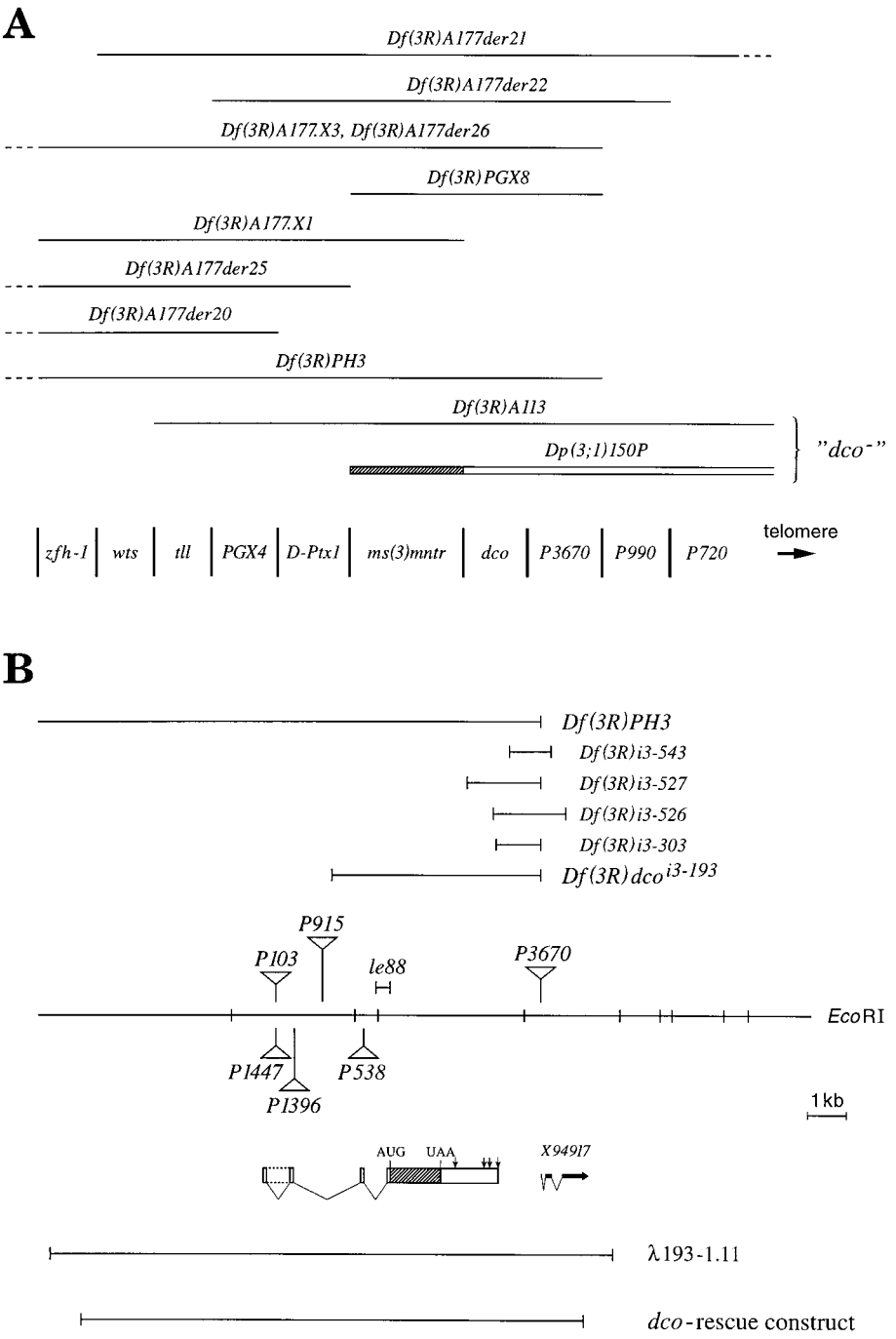

Fig. 6. Map and structural organization of the *dco* gene. (A) Genetic map of the *dco* locus. Deficiencies have been mapped with respect to *dco*, the previously mapped loci *zfh-1*, *wts*, *tll*, *PGX4* (Justice et al., 1995), *D-Ptx1* (Vorbrüggen et al., 1997), and the lethal P-element insertions *P990* (Deák et al., 1997), *P3670*, and *P720* (kindly provided by the Berkeley Drosophila Genome Project). Possible proximal and distal extensions of the deficiencies are indicated by broken lines. The distal breakpoints of *Df(3R)A177der20* and *Df(3R)A177der25*, and the proximal breakpoint of *Df(3R)A177der22* have been mapped more precisely earlier (Vorbrüggen et al., 1997) while the proximal breakpoints of *Df(3R)PGX8* and *Dp(3;1)150P* map within less than 5 kb of and less than 20 kb distal to the distal breakpoint of *Df(3R)A177der25*, respectively. *Df(3R)PGX8* (kindly provided by J. Lengyel) and *Df(3R)A177.X1* do not fully complement since *Df(3R)PGX8/Df(3R)A177.X1* males are sterile, which identifies a new male sterile locus named *male sterile minotaurus* (*ms(3)mntr*). The synthetic deficiency *Df(3R)A113 Dp(3;1)150P* carries a *dco* gene inactivated through heterochromatization by juxtaposed sex chromosome heterochromatin (see Materials and methods). (B) Structural organization of the *dco* transcription unit. The intron-exon structure of the *dco* gene and of the adjacent *X94917* transcription unit (Berkeley Drosophila Genome Project) are shown with respect to a genomic *Eco*RI restriction map above and the insert of phage λ193-1.11 isolated from a genomic library in λDASH II. The open reading frame of *dco*, located in the last exon, is indicated as hatched box while several of its polyA addition sites are marked by vertical arrows above the last exon. The first intron frequently remains unspliced in cDNAs isolated from embryonic libraries as indicated by dotted lines. The breakpoints of several small deficiencies and the distal breakpoint of the large deficiency *Df(3R)PH3*, which is also shown in A, and the sites of several P-element insertions have been mapped by DNA sequencing and are shown with respect to the *Eco*RI map. The extent of the genomic region used in a P-element mediated rescue construct, which rescues all *dco* alleles and the insertion mutant *P3670* of the *X94917* gene, is illustrated at the bottom.

(Deák et al., 1997), *P{ry$^{+t7.2}$=PZ}l(3)720* (*P720*), and *P{ry$^{+t7.2}$=PZ}l(3)3670* (*P3670*). Subsequently, the *dco* gene was reduced to a small deficiency, *Df(3R)dco$^{i3\text{-}193}$*, generated by imprecise excision of the P element *P3670*, and DNA including the entire gene was cloned as a single insert from a genomic library as illustrated in Fig. 6B and described in the Appendix (available in online version). Several cDNAs, all derived from the *dco* transcript, were isolated and mapped with respect to the genomic DNA by sequencing (Fig. 6B).

The identity of the *dco* transcript was corroborated by mapping the insertion sites of several P-element alleles of *dco*, obtained by mobilization of *P3670* or by screening a collection of P-element insertions on the third chromosome (Deák et al., 1997) for lack of complementation with *dco*. These insertions are located in the first two introns and in the 5′ donor splice site of the third intron (Fig. 6B). Finally, all *dco* alleles, including *dco^3*, are completely rescued by a *dco* transgene consisting of a 13 kb genomic fragment which includes the entire *dco* transcription unit as well as flanking sequences (Fig. 6B). This shows clearly that all of the tested mutations are bona fide *dco* alleles and that none is a mutant allele of a gene different from, but interacting with, *dco*. In particular, as homozygous *dco^3* larvae can be rescued by a

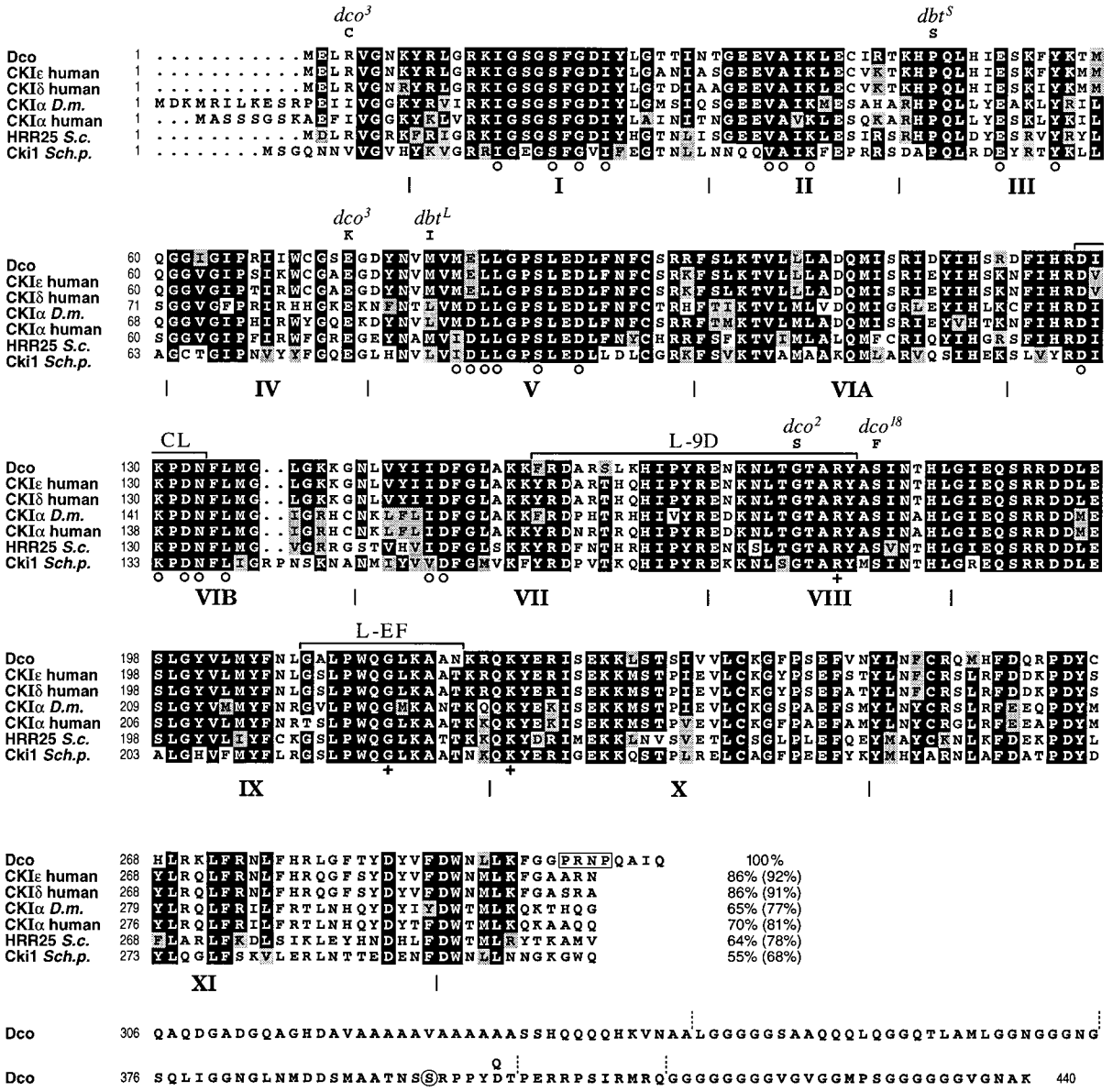

Fig. 7. Comparison of catalytic domains of Dco and other CKI proteins from Yeast, *Drosophila* and Humans, and characterization of Dco point mutations. The predicted amino acid sequence of Dco is shown, and its kinase domain is compared to those of human CKIε and δ (Fish et al., 1995), *Drosophila* (Santos et al., 1996) and human CKIα (Tapia et al., 1994), and to those of its yeast homologs, HRR25 of *Saccharomyces cerevisiae* (Hoekstra et al., 1991) and Cki1 of *Schizosaccharomyces pombe* (Wang et al., 1994). At the end of the catalytic domains the identity (and similarity) of their amino acid sequences with respect to that of Dco are listed. Missense mutations in dco^2, dco^{18} and dco^3 are identified and those of the two *dbt* alleles (Kloss et al., 1998) are indicated. The polymorphism D401Q is found in dco^2, dco^3 and *dbt* (Kloss et al., 1998). The limits of the 12 subdomains of the catalytic domain (Roman numerals; Hanks and Hunter, 1995), are indicated below their sequence by vertical lines. Residues directly or indirectly participating in ATP binding (o) and those thought to recognize the phosphate group (+) of the putative substrate recognition site (S(P)-X-X-S/T) are suggested by the highly conserved 3-D structure of the catalytic domain in crystals (Xu et al., 1995; Longenecker et al., 1996). In addition, the L-9D and L-EF loops, thought to be involved in substrate recognition and the control of CKI activity (Xu et al., 1995), and the catalytic loop (CL) are marked by brackets. A potential SH3-binding motif is boxed, and a possible autophosphorylation site in the C-terminal domain is circled. Dotted vertical lines subdivide the C-terminal domain of Dco into ala/gln-rich (301-345), gly-rich (346-375), ser/thr-rich (376-402), arg-rich (403-413), and very gly-rich (414-440) subdomains. The GenBank accession number for the nucleotide and amino acid sequence of the *dco* gene and its mutant alleles is AF192484.

single copy of a dco^+ transgene to fully viable and fertile wild-type adults, dco^3 is clearly a loss-of-function allele.

The *dco* gene encodes a homolog of human CKIε and δ

Genomic and cDNA sequence analysis showed that the transcribed portion of *dco* consists of four exons and three introns (Fig. 6B). The first intron frequently remains unspliced despite the use of two closely spaced alternative 5′ donor splice sites. Surprisingly, all introns reside in the region corresponding to the untranslated leader whereas the last exon contains the entire coding region. The longest open reading

frame encodes a protein of 440 amino acids, of which the 300 N-terminal amino acids have a high level of sequence identity with the catalytic domain of members of the CKI family (Fig. 7). The most closely related isoforms are human CKIε and δ with 86% sequence identity (both isoforms) and 92% or 91% similarity, respectively, through the kinase domain. Even when compared to CKI isoforms of lower eukaryotes, such as HRR25 of budding yeast (78% similarity) or Cki1 and Cki2 of fission yeast (68% similarity), the catalytic domain of Dco is highly conserved (Fig. 7). The ultimate evidence for the extreme structural conservation of the catalytic domain of CKI proteins, at least among members of the CKIδ/ε subfamily, comes from a comparison of their 3-D structures at 2 Å resolution, which shows that the yeast and human isoforms are nearly identical (Xu et al., 1995; Longenecker et al., 1996). This allows us to interpret the effects of *dco* mutations in the catalytic domain in terms of these known 3-D structures from yeast and humans (see Appendix).

The 140 amino-acid C-terminal domain of Dco (Fig. 7) is not conserved among CKIδ/ε subfamily members (Rowles et al., 1991). However, these domains do share the feature of consisting predominantly of regions that are abnormally rich in a few amino acids. In addition, they encompass several potential phosphorylation sites, including a site for autophosphorylation and a short arg-rich stretch, possibly serving as a nuclear localization signal. A potential SH3-binding motif in the C-terminal domain of the CKIδ/ε subfamily (Hoekstra et al., 1991; Fish et al., 1995) appears to be conserved in Dco (Fig. 7).

The molecular lesions of the *dco* mutant alleles that we have used (Figs 6B and 7) and their possible implications are described and discussed in the Appendix.

DISCUSSION

We have shown that the *dco* gene encodes a highly conserved homolog of the mammalian ser/thr protein kinase CKIδ/ε and is identical to the *Drosophila dbt* gene (Kloss et al., 1998). However, in contrast to the weak *dbt* alleles, which shorten or prolong the period of the circadian rhythm (Price et al., 1998), the strong and null *dco* alleles described here exhibit dramatic effects on cell proliferation, apoptosis, and growth arrest that are not observed for *dbt* alleles. Correspondingly, null mutants of the *dco* homolog in budding yeast, *hrr25*, also show dramatically reduced growth rates and aberrant cell morphologies (Hoekstra et al., 1991). This seems particularly relevant because it has been shown that not only is the 3-D structure of the enzyme highly conserved from yeast to mammals (Xu et al., 1995; Longenecker et al., 1996), but also that expression of mammalian CKIε rescues the slow-growth phenotype of *hrr25* null mutants (Fish et al., 1995). This high level of conservation suggests that *dco* may also have conserved functions similar to those of its budding yeast homolog. However, in addition to the functions described for yeast, the Dco kinase appears to play a role in growth arrest of imaginal discs and thus controls the size and shape of the adult structures to which they give rise. Because of the high structural and functional conservation, results obtained for *dco* in *Drosophila* are likely to be equally significant for higher organisms, including man.

The fact that *dco* encodes a ser/thr protein kinase, together with many aspects of its mutant phenotypes, suggests that the protein may function in one or more signal transduction pathways. All known protein kinases are regulated by external signals and regulate downstream components by phosphorylation. The activity of CKIδ/ε is known to be regulated by phosphorylation in other organisms (Graves and Roach, 1995; Rivers et al., 1998). Moreover, it has recently been shown that Cki1, the *S. pombe* homolog of CKIδ/ε (Fig. 7), inhibits phosphatidylinositol 4-phosphate 5-kinase (PIP5K) and hence the synthesis of phosphatidylinositol 4,5-bisphosphate (PIP_2) (Vancurova et al., 1999). PIP_2 itself is a second messenger as well as an important substrate of phospholipase C, which converts it to additional second messengers, activating, for example, protein kinase C. *skittles* (*sktl*), the gene encoding a *Drosophila* homolog of PIP5K, is required for cell viability and germline development (Hassan et al., 1998). Similarly, Dco functions are required for cell survival in imaginal discs as well as for germline development since females lay no eggs if their germline is homozygous for dco^{le88} on a chromosome free of other lethal mutations (E. F., unpublished results). Therefore, it is possible that Sktl is a substrate of Dco. If so, the level of PIP_2 would be regulated by Sktl and Dco in opposite ways and must be critical for these processes. In addition, the observation that the activity of mammalian CKIε can be regulated in vivo by autophosphorylation/dephosphorylation of its C-terminal domain (Rivers et al., 1998), suggests that one substrate of Dco might be Dco itself. Moreover, as phosphorylation of the C-terminal portion of CKIε inhibits the kinase activity (Rivers et al., 1998), this domain might well be the target of several signaling pathways regulating Dco activity. Lastly, Dco functions in a pathway controlling circadian rhythm, and in this case one of its substrates appears to be the Period (Per) protein (Price et al., 1998).

For *dbt* alleles no mutant adult phenotype other than the shortened or prolonged circadian rhythm has been reported (Kloss et al., 1998). Consistent with this mild phenotype, both *dbt* mutations are missense mutations at locations not expected to affect the catalytic site of the kinase domain (Fig. 7). They probably result in altered affinities for the protein substrate Per, which mediates their effect on the circadian rhythm. Similarly, none of the *dco* point mutations appears to affect the catalytic activity of the Dco kinase, consistent with the production by these mutations of a wide variety of mutant phenotypes (see Appendix and Fig. 7). While Per has been shown to be a substrate of Dco in vivo, the strong morphogenetic effects of Dco cannot be mediated only through Per because *per* null mutants are viable and show none of the *dco* phenotypes reported here (Lindsley and Zimm, 1992). For the elucidation of all functions of Dco, it will be important to find its additional substrates that might act in signal transduction pathways controlling cell survival, proliferation, and growth arrest.

Dco is required for both growth and growth arrest in discs

Analysis of *dco* mutant phenotypes shows that complete loss of *dco* function in heteroallelic combinations of null alleles is lethal during larval stages. Growth of imaginal discs, one of the main proliferating tissues during larval stages, is strongly inhibited in *dco* null mutants. Cells of these discs are able to

divide, possibly because of the perdurance of maternal Dco protein, but degenerate after only few divisions. Surprisingly, despite this strong inhibition of growth and survival of imaginal discs, many larvae survive to the third instar, which is often prolonged by more than two weeks at 25°C before the larvae die. Weaker *dco* alleles (*dco*^{2}, *dco*^{P1396} and *dco*^{P915}) appear to result in reduced growth rates of discs and death during late larval or early pupal stages, while heteroallelic combinations with weak alleles (*dco*^{P103} and *dco*^{P1447}) die as pharate adults or survive to viable adults. Surprisingly, one allele, *dco*^{3}, displays the opposite phenotype, i.e., its heteroallelic combinations show excess cell proliferation in imaginal discs.

Growth inhibition and apoptosis is also observed in *dco*$^{-}$ clones and this phenotype is cell-autonomous, which suggests that *dco*$^{-}$ cells are unable to receive a signal that promotes cell growth or survival. In imaginal discs, growth is determined by cellular growth rather than cell proliferation, since progression through the cell cycle is tightly coupled to and depends on cell growth (Weigmann et al., 1997; Neufeld et al., 1998). Growth is regulated directly by signals including insulin, and indirectly by patterning signals including Dpp, Wg, and Notch (Lecuit et al., 1996; Nellen et al., 1996; Neumann and Cohen, 1996; Zecca et al., 1996; Horsfield et al., 1998; Johnston and Edgar, 1998; for reviews, see Edgar and Lehner, 1996; Serrano and O'Farrell, 1997). Both growth and patterning signals are essential for growth of discs as documented by the growth failure in clones mutant for the transduction of the Dpp or Wg signal (Burke and Basler, 1996; Orsulic and Peifer, 1996) and by the small disc phenotype of hypomorphic *insulin receptor* (*inr*) mutants (Chen et al., 1996). Evidently, Dco is not essential for the transduction of the Dpp patterning signal, since the activity of Dpp target genes is not altered in *dco*$^{-}$ clones, whereas Dco does appear to be required for the transduction of a growth or survival signal.

Although *dco* plays an essential role in growth and proliferation, this is not its sole morphogenetic function in imaginal discs. In general, mutant *dco* alleles inhibit growth of discs in homozygous and transheterozygous combinations. However, one allele, *dco*^{3}, hardly inhibits growth, if at all, but rather fails to arrest growth of discs when they have reached their normal size. Since *dco*^{3} animals can be rescued completely to wild type by a single *dco*$^{+}$ transgene, the failure in growth arrest of *dco*^{3} discs corresponds to a loss of function. As this property of *dco*^{3} is further cell-autonomous in clones, we conclude that the ability of *dco*^{3} cells to transduce a signal, required to stop growth at the end of larval life, is significantly reduced while the generation of the signal is not affected. Differentiation of *dco*^{3} animals to pharate adults (Fig. 2) implies that growth arrest of *dco*^{3} discs is only delayed but not abolished, which indicates that Dco^{3} is hypomorphic for the growth arrest function of Dco.

The foregoing interpretation of Dco functions is also consistent with the observation that transheterozygous combinations of *dco*^{3} with *dco* alleles that are hypomorphic or amorphic for the Dco growth or survival function show disc overgrowth, if these alleles are also hypomorphic for the Dco growth-arrest function, a condition met by all null and most P alleles. Our analysis of *dco*^{3} transheterozygotes suggests that the two point alleles, *dco*^{2} and *dco*^{18}, are also hypomorphic for the disc overgrowth phenotype. We further infer from *dco*^{3} mutants that some features of the Dco CKI protein are essential only for the transduction of the growth arrest, but not of the growth or survival signal. It remains to be shown if complementary mutations of Dco can be generated that affect only its growth or survival but not its growth-arrest function. Such mutations over *dco*^{3} would complement to produce wild-type flies.

Homo- or hemizygous *dco*^{3} discs continue to grow and reach a size considerably larger than that of normal discs. This overgrowth is accompanied by massive apoptosis and a prolonged larval life. Apparently, larval life continues as long as growth of imaginal discs has not been arrested, which suggests a coupling of pupariation to growth arrest of discs and is consistent with an earlier proposal (Simpson et al., 1980). Moreover, while larval disc cells that fail to proliferate undergo apoptosis, this fate is suppressed in non-dividing pupal cells. Apoptosis in overgrowing *dco*^{3} discs indicates that it may be induced in regions of hyperplastic growth as well. Apoptosis followed by intercalary growth in discs probably also gives rise to the duplications and triplications observed in hemizygous *dco*^{3} pharate adults as well as the outgrowths and patterning phenotypes found in *dco* mutants that survive to adulthood (French et al., 1976). The more dramatic *dco*^{3} phenotypes might result from excessive intercalary growth in these mutants.

We conclude that Dco is part of at least two signal transduction pathways of disc morphogenesis, one responding to a growth or survival signal, the other to a signal that arrests growth when a disc has reached its normal size.

Regulation of Dco activity by growth or survival factors

It is evident from the discless phenotype of strong *dco* mutants and from the analysis of *dco* null clones, that cells in which Dco function has been sufficiently reduced die after only a few cell divisions. As cell growth and inhibition of apoptosis are thought to be intimately linked (Evan et al., 1995), these phenotypes can be explained by loss of function in either cell growth or cell survival, and wild-type Dco might function by stimulating growth and proliferation or by inhibiting apoptosis. Coupling of cell growth and survival could occur intracellularly through branched pathways activated by the same extracellular signal, for example insulin, or extracellularly through two distinct, but coordinately expressed, signals like insulin and a survival factor. One of the substrates of mammalian delta and epsilon isoforms of CKI is the tumor suppressor p53, which regulates both proliferation and apoptosis (Knippschild et al., 1997). Such a mechanism could be operating in *Drosophila*, although a fly counterpart of p53 is not yet known.

It is unclear which growth factors may regulate the activity of Dco. The main growth factor known to be required for growth of imaginal discs is insulin (Cullen and Milner, 1991), and hypomorphic *inr* mutants show small disc phenotypes similar to those of hypomorphic *dco* larvae (Chen et al., 1996). But whereas some *dco* phenotypes resemble *inr* phenotypes, strong *inr* mutants die during embryogenesis (Fernandez et al., 1995; Chen et al., 1996). In contrast, *dco* null mutants develop to third-instar larvae and may survive for as long as three weeks at 25°C. Therefore, if Dco activity is regulated by the insulin pathway, it may function in only some but not all of its branched pathways (Yenush et al., 1996).

In addition to insulin, a family of growth factors required for growth of imaginal discs has recently been identified (Kawamura et al., 1999). These IDGFs (Imaginal Disc Growth Factors) are produced in the larval fat body and support survival of disc cells in culture, but are also necessary, in combination with insulin, for proliferation (Kawamura et al., 1999). Perhaps Dco reacts to these factors or even serves to integrate insulin and IDGF signals. It is thus conceivable that Dco activity in discs depends on both type of signals, which might explain the similarity of hypomorphic *inr* and *dco* disc phenotypes. It is also possible that recognition of some substrates by Dco requires both signals, while its recognition of other substrates depends on only one of them. That Dco is probably a component of several distinct pathways is further suggested by its additional role in the circadian rhythm (Kloss et al., 1998; Price et al., 1998).

It should be emphasized that growth and survival of most larval tissues does not depend on Dco. Hence, *dco* null mutants are able to survive as discless third-instar larvae for a very long time. Most of them are unable to pupariate, probably because pupariation is coupled to the arrest of overall disc proliferation when discs have reached their normal size. We may thus speculate and consider *dco* as an atavistic mutation because it prevents metamorphosis of the larval worm and considerably prolongs its life span. In *C. elegans* mutations in the insulin pathway are known to result in the formation of a developmentally arrested larval form that can survive for a long time, the dauer larva (for a review see Wood, 1998). It is thus tempting to speculate that the considerably extended larval life span of *dco* null mutants might have a similar cause.

We are grateful to Konrad Basler for discussions and experimental advice, to Yu Zou for help in P-element transformations, to Judy Lengyel and Peter Deák for *Drosophila* mutants, to Werner Boll, Michael Daube and Catherine Saner for DNA sequencing, and to Fritz Ochsenbein for excellent artwork. We thank Konrad Basler, Hans Noll and Joy Alcedo for discussions and comments on the manuscript. This work has been supported by grant CA69108 from the National Institutes of Health (to P. J. B.), grant 31-40874.94 from the Swiss National Science Foundation (to M. N.), and by the Kanton Zürich.

REFERENCES

Burke, R. and Basler, K. (1996). Dpp receptors are autonomously required for cell proliferation in the entire developing *Drosophila* wing. *Development* **122**, 2261-2269.

Campbell, G. and Tomlinson, A. (1999). Transducing the Dpp morphogen gradient in the wing of *Drosophila*: regulation of Dpp targets by *brinker*. *Cell* **96**, 553-562.

Chen, C., Jack, J. and Garofalo, R. S. (1996). The *Drosophila* insulin receptor is required for normal growth. *Endocrinology* **137**, 846-856.

Cullen, C. F. and Milner, M. J. (1991). Parameters of growth in primary cultures and cell lines established from *Drosophila* imaginal discs. *Tissue Cell* **23**, 29-39.

Deák, P., Omar, M. M., Saunders, R. D. C., Pál, M., Komonyi, O., Szidonya, J., Maróy, P., Zhang, Y., Asburner, M., Benos, P., Savakis, C., Sidén-Kiamos, I., Louis, C., Bolshakov, V. N., Kafatos, F. C., Madueno, E., Modolell, J. and Glover, D. M. (1997). *P*-element insertion alleles of essential genes on the third chromosome of *Drosophila melanogaster*: Correlation of physical and cytogenetic maps in chromosomal region 86E-87F. *Genetics* **147**, 1697-1722.

Edgar, B. E. and Lehner, C. F. (1996). Developmental control of cell cycle regulators: a fly's perspective. *Science* **274**, 1646-1652.

Evan, G. I., Brown, L., Whyte, M. and Harrington, E. (1995). Apoptosis and the cell cycle. *Curr. Opin. Cell. Biol*. **7**, 825-834.

Fernandez, R., Tabarini, D., Azpiazu, N., Frasch, M. and Schlessinger, J. (1995). The *Drosophila* insulin receptor homolog: a gene essential for embryonic development encodes two receptor isoforms with different signaling potential. *EMBO J*. **14**, 3373-3384.

Fish, K. J., Cegielska, A., Getman, M. E., Landes, G. M. and Virshup, D. M. (1995). Isolation and characterization of human casein kinase Iε (CKI), a novel member of the CKI gene family. *J. Biol. Chem*. **270**, 14875-14883.

Frei, E., Baumgartner, S., Edström, J.-E. and Noll, M. (1985). Cloning of the *extra sex combs* gene of *Drosophila* and its identification by P-element-mediated gene transfer. *EMBO J*. **4**, 979-987.

French, V., Bryant, P. J. and Bryant, S. V. (1976). Pattern regulation in epimorphic fields. *Science* **93**, 969-981.

Frisardi, M. C. and MacIntyre, R. J. (1984). Position effect variegation of an acid phosphatase gene in *Drosophila melanogaster*. *Mol. Gen. Genet.* **197**, 403-413.

Fu, W. and Noll, M. (1997). The *Pax2* homolog *sparkling* is required for development of cone and pigment cells in the *Drosophila* eye. *Genes Dev*. **11**, 2066-2078.

Graves, P. R. and Roach, P. J. (1995). Role of COOH-terminal phosphorylation in the regulation of casein kinase Iδ. *J. Biol. Chem*. **270**, 21689-21694.

Hanks, S. K. and Hunter, T. (1995). The eukaryotic protein kinase superfamily: kinase (catalytic) domain structure and classification. *FASEB J*. **9**, 576-596.

Hassan, B. A., Prokopenko, S. N., Breuer, S., Zhang, B., Paululat, A. and Bellen, H. J. (1998). *skittles*, a Drosophila phosphatidylinositol 4-phosphate 5-kinase, is required for cell viability, germline development and bristle morphology, but not for neurotransmitter release. *Genetics* **150**, 1527-1537.

Hoekstra, M. F., Liskay, R. M., Ou, A. C., DeMaggio, A. J., Burbee, D. G. and Heffron, F. (1991). HRR25, a putative protein kinase from budding yeast: association with repair of damaged DNA. *Science* **253**, 1031-1034.

Horsfield, J., Penton, A., Secombe, J., Hoffman, F. M. and Richardson, H. (1998). *decapentaplegic* is required for arrest in G_1 phase during *Drosophila* eye development. *Development* **125**, 5069-5078.

Jiang, J. and Struhl, G. (1996). Complementary and mutually exclusive activities of Decapentaplegic and Wingless organize axial patterning during *Drosophila* leg development. *Cell* **86**, 401-409.

Johnston, L. A. and Edgar, B. A. (1998). Wingless and Notch regulate cell-cycle arrest in the developing *Drosophila* wing. *Nature* **394**, 82-84.

Jursnich, V. A., Fraser, S. E., Held, L. I., Jr., Ryerse, J. and Bryant, P. J. (1990). Defective gap-junctional communication associated with imaginal disc overgrowth and degeneration caused by mutations of the *dco* gene in *Drosophila*. *Dev. Biol*. **140**, 413-429.

Justice, R. W., Zilian, O., Woods, D. F., Noll, M. and Bryant, P. J. (1995). The *Drosophila* tumor suppressor gene *warts* encodes a homolog of human myotonic dystrophy kinase and is required for the control of cell shape and proliferation. *Genes Dev*. **9**, 534-546.

Kankel, D. R. and Hall, J. C. (1976). Fate mapping of nervous system and other internal tissues in genetic mosaics of *Drosophila melanogaster*. *Dev. Biol*. **48**, 1-24.

Kawamura, K., Shibata, T., Saget, O., Peel, D. and Bryant, P. J. (1999). A new family of growth factors produced by the fat body and active on *Drosophila* imaginal disc cells. *Development* **126**, 211-219.

Kilchherr, F., Baumgartner, S., Bopp, D., Frei, E. and Noll, M. (1986). Isolation of the *paired* gene of *Drosophila* and its spatial expression during early embryogenesis. *Nature* **321**, 493-499.

Kloss, B., Price, J. L., Saez, L., Blau, J., Rothenfluh, A., Wesley, C. S. and Young, M. W. (1998). The *Drosophila* clock gene *double-time* encodes a protein closely related to human casein kinase Iε. *Cell* **94**, 97-107.

Knippschild, U., Milne, D. M., Campbell, L. E., DeMaggio, A. J., Christenson, E., Hoekstra, M. F. and Meek, D. W. (1997). p53 is phosphorylated in vitro and in vivo by the delta and epsilon isoforms of casein kinase 1 and enhances the level of casein kinase 1 delta in response to topoisomerase-directed drugs. *Oncogene* **15**, 1727-1736.

Kongsuwan, K., Dellavalle, R. P. and Merriam, J. R. (1986). Deficiency analysis of the tip of chromosome *3R* in *Drosophila melanogaster*. *Genetics* **112**, 539-550.

Lecuit, T., Brook, W. J., Ng, M., Calleja, M., Sun, H. and Cohen, S. M. (1996). Two distinct mechanisms for long-range patterning by Decapentaplegic in the *Drosophila* wing. *Nature* **381**, 387-393.

Lindsley, D. L., Edington, C. W. and von Halle, E. S. (1960). Sex-linked recessive lethals in *Drosophila* whose expression is suppressed by the Y chromosome. *Genetics* **45**, 1650-1670.

Lindsley, D. L. and Zimm, G. G. (1992). The Genome of *Drosophila melanogaster*. San Diego, California: Academic Press.

Longenecker, K. L., Roach, P. J. and Hurley, T. D. (1996). Three-dimensional structure of mammalian casein kinase I: Molecular basis for phosphate recognition. *J. Mol. Biol*. **257**, 618-631.

Madhavan, M. M. and Schneiderman, H. A. (1977). Histological analysis of the dynamics of growth of imaginal discs and histoblast nests during the larval development of *Drosophila melanogaster*. *Roux's Arch. Dev. Biol*. **183**, 269-305.

Maniatis, T., Fritsch, E.F. and Sambrook, J. (1982). *Molecular Cloning: A Laboratory Manual.* Cold Spring Harbor Laboratory Press, Cold Spring Harbor, NY.

Morata, G. and Ripoll, P. (1975). Minutes: mutants of Drosophila autonomously affecting cell division rate. *Dev. Biol.* **42**, 211-221.

Nellen, D., Burke, R., Struhl, G. and Basler, K. (1996). Direct and long-range action of a DPP morphogen gradient. *Cell* **85**, 357-368.

Neufeld, T. P., de la Cruz, A. F. A., Johnston, L. A. and Edgar, B. A. (1998). Coordination of growth and cell division in the *Drosophila* wing. *Cell* **93**, 1183-1193.

Neumann, C. J. and Cohen, S. M. (1996). Distinct mitogenic and cell fate specification functions of *wingless* in different regions of the wing. *Development* **122**, 1781-1789.

O'Brochta, D. and Bryant, P. J. (1983). Cell degeneration and elimination in the imaginal wing disc, caused by the mutations *vestigial* and *ultravestigial* of *Drosophila melanogaster*. *Roux's Arch. Dev. Biol*. **192**, 285–294.

Orsulic, S. and Peifer, M. (1996). An in vivo structure-function study of Armadillo, the β-Catenin homologue, reveals both separate and overlapping regions of the protein required for cell adhesion and for Wingless signaling. *J. Cell Biol*. **134**, 1283-1300.

Pignoni, F., Baldarelli, R. M., Steingrímsson, E., Diaz, R. J., Patapoutian, A., Merriam, J. R. and Lengyel, J. A. (1990). The *Drosophila* gene *tailless* is expressed at the embryonic termini and is a member of the steroid receptor superfamily. *Cell* **62**, 151-163.

Pirrotta, V. (1986). Cloning *Drosophila* genes. In *Drosophila: A Practical Approach*. (ed. D. B. Roberts) Oxford: IRL Press Limited.

Price, J. L., Blau, J., Rothenfluh, A., Abodeely, M., Kloss, B. and Young, M. W. (1998). *double-time* is a novel *Drosophila* clock gene that regulates PERIOD protein accumulation. *Cell* **94**, 83-95.

Rivers, A., Gietzen, K. F., Vielhaber, E. and Virshup, D. M. (1998). Regulation of casein kinase I ε and casein kinase I δ by an in vivo futile phosphorylation cycle. *J. Biol. Chem*. **273**, 15980-15984.

Robertson, H. M., Preston, C. R., Phillis, R. W., Johnson-Schlitz, D. M., Benz, W. K. and Engels, W. R. (1988). A stable genomic source of P element transposase in *Drosophila melanogaster*. *Genetics* **118**, 461-470.

Rowles, J., Slaughter, C., Moomaw, C., Hsu, J. and Cobb, M. H. (1991). Purification of casein kinase I and isolation of cDNAs encoding multiple casein kinase I-like enzymes. *Proc. Natl. Acad. Sci. USA* **88**, 9548-9552.

Santos, J. A., Logarinho, E., Tapia, C., Allende, C. C., Allende, J. E. and Sunkel, C. E. (1996). The casein kinase 1α gene of *Drosophila melanogaster* is developmentally regulated and the kinase activity of the protein induced by DNA damage. *J. Cell Sci*. **109**, 1847-1856.

Serrano, N. and O'Farrell, P. H. (1997). Limb morphogenesis: connections between patterning and growth. *Curr. Biol.* **7**, R186-R195.

Simpson P. (1979). Parameters of cell competition in the compartments of the wing disc of *Drosophila*. *Dev. Biol*. **69**, 182-193.

Simpson, P., Berreur, P. and Berreur-Bonnenfant, J. (1980). The initiation of pupariation in *Drosophila*: dependence on growth of the imaginal discs. *J. Embryol. Exp. Morph*. **57**, 155-165.

Strecker, T. R., Merriam, J. R. and Lengyel, J. A. (1988). Graded requirement for the zygotic terminal gene, *tailless*, in the brain and tail region of the *Drosophila* embryo. *Development* **102**, 721-734.

Sun, Y. H., Tsai, C.-J., Green, M. M., Chao, J.-L., Yu, C.-T., Jaw, T. J., Yeh, J.-Y. and Bolshakov, V. N. (1995). *white* as a reporter gene to detect transcriptional silencers specifying position-specific gene expression during *Drosophila melanogaster* eye development. *Genetics* **141**, 1075-1086.

Tapia, C., Featherstone, T., Gómez, C., Taillon-Miller, P., Allende, C. C. and Allende J. E. (1994). Cloning and chromosomal localization of the gene coding for human protein kinase CK1. *FEBS Lett*. **349**, 307-312.

Theisen, H., Haerry, T. E., O'Connor, M. B. and Marsh, J. L. (1996). Developmental territories created by mutual antagonism between Wingless and Decapentaplegic. *Development* **122**, 3939-3948.

Thummel, C. S. and Pirrotta, V. (1992). New pCasPeR P-element vectors. *Dros. Inf. Serv*. **71**, 150.

Tower, J., Karpen, G. H., Craig, N. and Spradling, A. C. (1993). Preferential transposition of *Drosophila* P elements to nearby chromosomal sites. *Genetics* **133**, 347-359.

Vancurova, I., Choi, J. H., Lin, H., Kuret, J. and Vancura, A. (1999). Regulation of phosphatidylinositol 4-phosphate 5-kinase from *Schizosaccharomyces pombe* by casein kinase I. *J. Biol. Chem*. **274**, 1147-1155.

Vorbrüggen, G., Constien, R., Zilian, O., Wimmer, E. A., Dowe, G., Taubert, H., Noll, M. and Jäckle, H. (1997). Embryonic expression and characterization of a Ptx1 homolog in *Drosophila*. *Mech. Dev*. **68**, 139-147.

Wang, P.-C., Vancura, A., Desai, A., Carmel, G. and Kuret, J. (1994). Cytoplasmic forms of fission yeast casein kinase-1 associate primarily with the particulate fraction of the cell. *J. Biol. Chem*. **269**, 12014-12023.

Weigmann, K., Cohen, S. M. and Lehner, C. F. (1997). Cell cycle progression, growth and patterning in imaginal discs despite inhibition of cell division after inactivation of *Drosophila* Cdc2 kinase. *Development* **124**, 3555-3563.

Wood, W. B. (1998). Aging of *C. elegans*: Mosaics and mechanisms. *Cell* **95**, 147-150.

Xu, R.-M., Carmel, G., Sweet, R. M., Kuret, J. and Cheng, X. (1995). Crystal structure of casein kinase-1, a phosphate-directed protein kinase. *EMBO J*. **14**, 1015-1023.

Xu, T. and Rubin, G.M. (1993). Analysis of genetic mosaics in developing and adult *Drosophila* tissues. *Development* **117**, 1223-1237.

Yenush, L., Fernandez, R., Myers, M. G., Jr., Grammer, T. C., Sun, X. J., Blenis, J., Pierce, J. H., Schlessinger, J. and White, M. F. (1996). The *Drosophila* insulin receptor activates multiple signaling pathways but requires insulin receptor substrate proteins for DNA synthesis. *Mol. Cell. Biol*. **16**, 2509-2517.

Zecca, M., Basler, K. and Struhl, G. (1996). Direct and long-range action of a Wingless morphogen gradient. *Cell* **87**, 833-844.

Zhang, P. and Spradling, A.C. (1993). Efficient and dispersed local *P* element transposition from *Drosophila* females. *Genetics* **133**, 361-373.

Appendix

Mapping and isolation of the *dco* locus

Since *dco* and *P3670* complement each other but are not separated by any deficiency breakpoints (Fig. 6A), an attempt was made to determine the physical distance between these two loci by recombination mapping. Among about 20,000 progeny, no recombinants were found, which suggests that *dco* and *P3670* are separated by less than 9 kb (Bender et al., 1983).

Taking advantage of the close proximity between *P3670* and *dco*, we screened for small deficiencies generated by transposase mediated P-element mobilization. After mobilizing *P3670*, the offspring were screened for the loss of the ry^+ eye marker carried by the P element. Such ry^- flies were further scored for homozygous lethality and for lack of complementation with their original P-element insertion and *dco*. As a result, several different imprecise excisions were recovered six of which are shown in Fig. 6B. All of these imprecise excisions do not complement *P3670* but complement *dco*, with the exception of (i) *Df(3R)PH3*, which is a large deficiency deleting several loci proximal to *P3670* (Fig. 6A) and thus maps *dco* proximal to *P3670* on the chromosome, and (ii) $Df(3R)dco^{i3\text{-}193}$, which is unusual because it complements the P-element insertion *P3670*, from which it has been generated, but does not complement *dco*.

After reducing the region harboring the *dco* gene to a small deficiency, DNA fragments flanking the P-element insertion *P3670* were isolated by plasmid rescue and used as probe to isolate phage λ193-1.11 from a genomic library (Fig. 6B). Analysis by whole genome Southern blots confirmed that $Df(3R)dco^{i3\text{-}193}$ was indeed a relatively small deficiency affecting four adjacent *Eco*RI fragments of 3.2, 0.6, 3.8 and 2.5 kb. Using these fragments as probes, 15 cDNAs were isolated from an embryonic cDNA library, which were all derived from a single transcription unit spanning the 3.2, 0.6 and 3.8 kb fragments (Fig. 6B). Comparison of genomic and cDNA sequences revealed that the 3′ end of the longest cDNA is still 1.12 kb upstream from *P3670*, which affects a transcript that extends distally (Fig. 6B), raising the possibility that *dco* is located within this 1.12 kb region and is not encoded by the isolated cDNAs. However, this possibility was ruled out since several of the previously obtained imprecise excisions of *P3670*, which complemented *dco* but failed to complement *P3670*, deleted this entire region, including part of the untranslated trailer (Fig. 6B). Therefore, the isolated cDNAs are all derived from the *dco* transcript.

Characterization of molecular lesions in *dco* mutant alleles

The various *dco* alleles listed in Table 1 show a wide range of phenotypes as illustrated in Figs 1-5. It was therefore of interest to know by which molecular lesions these were generated to provide some insight into the mechanisms that might be involved. To this end, all EMS-induced alleles, dco^2, dco^3, dco^{18} and dco^{le88}, were isolated from genomic libraries, and their exons and intron/exon boundaries were sequenced. Comparison with the wild-type *dco* DNA sequence shows that dco^{le88} is a 369 bp deficiency which deletes the last intron/exon boundary and ends after the T of the ATG initiation codon. In contrast, dco^2 and dco^{18} are true point mutations in the catalytic domain, resulting in the replacement of single amino acids, G175S in dco^2 and S181F in dco^{18}, that are strictly conserved in, and specific for, the CKI kinase family (Fig. 7). The dco^3 allele reveals two point mutations in the catalytic domain that give rise to the missense mutations R4C and E74K (Fig. 7). While the first mutation occurs very close to the N terminus in a residue that is not conserved in the CKIδ/ε subfamily and thus might not affect the wild-type structure, the second mutation is expected to have a strong effect since it alters a strictly conserved acidic into a basic amino acid. A third mutation in the amino acid sequence of dco^3, D401Q, in the C-terminal domain is a polymorphism without effect on the activity of Dco since the same alteration is found in the dco^2 allele which shares several additional polymorphisms with dco^3 that do not result in amino acid changes.

In addition to the analysis of the mutations in EMS-induced *dco* alleles, we determined the insertion sites of the P-element alleles by plasmid rescue and subsequent DNA sequencing. Surprisingly, two different P elements, *P103* and *P1447*, which can be distinguished by their resistance to different antibiotics, have inserted at the same site into the first 612 bp intron, 251 bp downstream from the 3′ end of exon 1. The chromosome carrying the *P103* insertion retained the lethal P-element insertion *P3670*, from which it has been derived by local hop, at its original location in the 5′ leader of the *X94917* transcript downstream of *dco* (Fig. 6B) and hence is also mutant for this adjacent lethal locus. Interestingly, the *dco*-rescue construct (Fig. 6B) also rescues the lethal *P3670* mutation since it extends 14 bp beyond the *X94917* coding region. Two P elements, *P1396* and *P915*, have inserted into the second intron of *dco*, 27 bp and 766 bp downstream of its 5′ end, respectively, and *P538* has inserted after the G of the GT donor splice site of the last intron.

Finally, we have sequenced the breakpoints of $Df(3R)dco^{i3\text{-}193}$, which deletes the second and third exon of *dco*, but complements the lethal insertion of *P3670*. The deficiency fuses the first 1005 bp of the 1747 bp second intron of *dco* to the first non-coding exon of the *X94917* transcript and thus expresses it under the control of the *dco* enhancer and promoter. The resulting *X94917* fusion gene is fully viable.

Effects of molecular lesions in *dco* alleles on allelic strength and phenotype

Since the 3-D structures of the catalytic domain of CKIδ/ε homologs have been highly conserved from yeast to mammals (Xu et al., 1995; Longenecker et al., 1996), we may assume that it has been conserved for Dco as well, which allows us to analyze the phenotypic consequences of the different mutations found in *dco* alleles in terms of their effect on the 3-D structure of Dco. The single point mutations in dco^2 and dco^{18} are not expected to affect the catalytic activity of Dco per se. Rather they both occur in a region known as the L-9D loop (Fig. 7). This loop and the L-EF loop have been suggested to play an important role in substrate recognition and in the control of kinase activity, either by regulating, through potential phosphorylation sites, the interaction with the protein substrate or by blocking, through an induced conformational change, the accessibility of the peptide substrate to the catalytic pocket close to the bound ATP (Xu et al., 1995; Longenecker et al., 1996). It is noteworthy that one of the three residues thought to be crucial for the interaction with the phosphate group in the phospho-serine/threonine (Xu et al., 1995; Longenecker et al.,

1996) of the CKI substrate recognition motif (Flotow et al., 1990) is located close to both mutations in the L-9D loop (Fig. 7). The S181F exchange in *dco*^{18} may be further deleterious for two reasons. (i) S181 forms a hydrogen bond to R193 (Xu et al., 1995) and is part of the SIN motif, which replaces in CKI the APE conserved in most other protein kinases; disruption of the hydrogen bond by F181 alters the protein surface, which is considered to be crucial for recognition of the protein substrate. (ii) S181 is a potential phosphorylation site whose phosphorylation would be a prerequisite for autophosphorylation at T184. Thus, an interpretation of the effect of *dco*^{2} and *dco*^{18} in terms of the 3-D structure of Dco suggests that they weaken or prevent the interaction with at least some of their protein substrates without affecting its catalytic activity. Alternatively, the *dco* point mutations might reduce the ability of Dco to serve itself as substrate for proteins regulating its activity. Phenotypic analysis suggests that *dco*^{18} is a very strong, possibly a null allele, while *dco*^{2} is strong, but clearly weaker. The small deficiency found in *dco*^{le88} suggests that it is a bona fide null allele because it deletes the last intron/exon boundary and part of the initiator codon.

The *dco*^{3} allele shows a rather drastic missense mutation, E74K, at a residue strictly conserved in all members of the CKIδ/ε subfamily. Since this residue is located within the surface thought to face the protein substrates and is not involved in the catalytic activity of the kinase domain, it might affect, similar to *dco*^{2} and *dco*^{18}, the interaction with a protein substrate. However, according to the specific *dco*^{3} overgrowth phenotype, in this case it would be a substrate essential for the transduction of the signal required to arrest rather than to promote growth of discs.

All of the P-element insertions that we have identified in *dco* are located in introns. The strongest of these *dco* alleles, *dco*^{P538}, destroys the 5′ splice site of the last intron and could only generate wild-type Dco kinase if splicing skipped the third exon. However, comparison with its phenotypes suggests that *dco*^{P538} might be a null allele and hence that such a splicing pattern is very inefficient, if it occurs at all. The strong *dco*^{P1396} allele has a P-element insertion close to the 5′ splice site of the second intron that might still strongly affect its splicing and thus result in much reduced Dco protein levels. It is clearly not a null allele, but stronger than the insertion *dco*^{P915} which occurred in the same intron and is probably removed by splicing with greater efficiency. The two weakest *dco* alleles are *dco*^{P103} and *dco*^{P1447}. Although they have inserted at precisely the same site of the first intron, *dco*^{P1447} is weaker and viable in combination with all other *dco* alleles. We assume that this difference in allelic strengths results from a difference in splicing efficiencies by which these two different P elements are removed from the *dco* transcript.

REFERENCES

Bender, W., Akam, M., Karch, F., Beachy, P. A., Peifer, M., Spierer, P., Lewis, E. B. and Hogness, D. S. (1983). Molecular genetics of the bithorax complex in *Drosophila melanogaster*. *Science* **221**, 23-29.

Flotow, H., Graves, P. R., Wang, A., Fiol, C. J., Roeske, R. W. and Roach, P. J. (1990). Phosphate groups as substrate determinants for casein kinase I action. *J. Biol. Chem.* **265**, 14264-14269.